

Energy and Delay Optimization for Cache-Enabled Dense Small Cell Networks

Hao Wu, Hancheng Lu

The Information Network Lab of EEIS Department USTC, Hefei, China, 230027

hwu2014@mail.ustc.edu.cn, hclu@ustc.edu.cn

Abstract—Caching popular files in small base stations (SBSs) has been proved to be an effective way to reduce bandwidth pressure on the backhaul links of dense small cell networks (DSCNs). Many existing studies on cache-enabled DSCNs attempt to improve user experience by optimizing end-to-end file delivery delay. However, under practical scenarios where files (e.g., video files) have diverse quality of service requirements, energy consumption at SBSs should also be concerned from the network perspective. In this paper, we attempt to optimize these two critical metrics in cache-enabled DSCNs. Firstly, we formulate the energy-delay optimization problem as a Mixed Integer Programming (MIP) problem, where file placement, user association and power control are jointly considered. To model the tradeoff relationship between energy consumption and end-to-end file delivery delay, a utility function linearly combining these two metrics is used as an objective function of the optimization problem. Then, we solve the problem in two stages, i.e. caching stage and delivery stage, based on the observation that caching is performed during off-peak time. At the caching stage, a local popular file placement policy is proposed by estimating user preference at each SBS. At the delivery stage, with given caching status at SBSs, the MIP problem is further decomposed by Benders' decomposition method. An efficient algorithm is proposed to approach the optimal association and power solution by iteratively shrinking the gap of the upper and lower bounds. Finally, extension simulations are performed to validate our analytical and algorithmic work. The results demonstrate that the proposed algorithms can achieve the optimal tradeoff between energy consumption and end-to-end file delivery delay.

Index Terms—Caching, Energy-delay optimization, File popularity, Dense small cell networks

I. INTRODUCTION

To cope with the explosive mobile traffic growth, dense small cell networks (DSCNs) are expected to be deployed in fifth generation (5G) cellular networks. In DSCNs, small base stations (SBSs) are usually connected to the core network via low-capacity backhaul links due to physical and cost-related limitations [1] [2]. That means the backhaul is prone to be the system bottleneck. Moreover, the backhaul problem becomes more serious as the SBS deployment density increases. Recently, enabling cache in DSCNs have been considered as a promising way to handle the backhaul problem [2]–[5]. Statistical report has shown that a few popular files requested by many users should account for most of backhaul traffic load [3]. Based on this fact, popular files can be proactively cached at SBSs, and delivered to users when requested, without consuming backhaul bandwidth. The effect of caching on the backhaul is determined by file reuse, i.e., the number of users

requesting the same file. If there is enough file reuse, caching can replace backhaul communication [2].

In cache-enabled DSCNs, user experience is also improved due to the reduction of end-to-end file delivery delay [1] [5]–[8]. When a user requests a file cached in the local SBS, the file is delivered by that SBS instead of the faraway Internet file server. In this case, end-to-end file delivery delay is significantly reduced. We can also see that minimizing end-to-end file delivery delay is equivalent to maximizing the cache hit ratio. Many existing studies attempt to improve the cache hit ratio by optimizing file placement in cache of SBSs [1] [2] [8]. However, the file placement optimization problem is non-trivial, which is coupled with the file popularity distribution (i.e., the probability that a file is requested by users) and user association strategy. When the file popularity distribution is known at each SBS, the file placement optimization problem can be converted to a well-known knapsack problem. Learning-based algorithm are proposed to obtain the file popularity profile and cache the best files at SBSs when the file popularity distribution is not known [1]. When users can associate with multiple SBSs, a distributed caching optimization problem is formulated based on a connectivity bipartite graph model and approximation algorithms that lie within a constant factor of the theoretical optimum are proposed [2]. In cache-enabled DSCNs with mobile users, the file replacement problem is optimized with recommendation via Q-learning [8].

Unlike end-to-end file delivery delay, energy consumption, which is widely concerned in 5G cellular networks [9], has not been well studied in cache-enabled DSCNs. There only exist a few studies on this issue. In [5], the impact of various factors (backhaul capacity, content popularity, cache capacity, etc.) on downlink energy efficiency (EE) is analyzed. It also validates that caching in DSCNs can achieve more EE gain compared with caching in conventional cellular networks. However, in this work, the user association strategy and quality of service (QoS) requirements from files are not considered. On the one hand, in DSCNs, multiple SBSs are available for a user that locates at the edge of a small cell. It means that the user have multiple association choices. In this case, the user association strategy has a significant impact on energy consumption [10] [11]. On the other hand, in practice, files have diverse QoS requirements. As we known, video traffic plays a major part in current mobile traffic, and is predicted to contribute over 80% of total mobile traffic in 2020 [12]. For online video delivery, the QoS requirement of each video file is usually expressed in

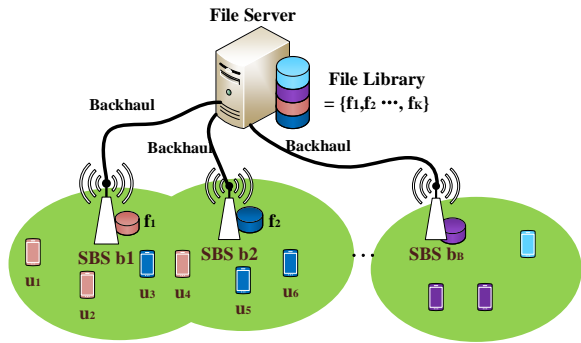


Fig. 1: Cache-enabled DSCNs.

forms of rate [13]. Consequently, different transmission power levels are configured at SBSs for video delivery to support required rates under various channel conditions.

Both end-to-end file delivery delay and energy consumption are critical metrics in cache-enabled DSCNs [14]. From the perspective of user experience, lower end-to-end file delivery delay are preferred, while less energy consumption is preferred from the network perspective. Unfortunately, there is a contradiction between these two metrics. Considering two SBSs, i.e., b_1 and b_2 , as well as their small cells described in Fig. 1, we assume that files have different QoS requirements in terms of rate. u_1, u_2 and u_4 request f_1 , and others request f_2 . To minimize end-to-end file delivery delay, the optimal user association strategy is: u_1, u_2 and u_4 associate with b_1 , others associate with b_2 . In this case, users can download files from SBSs, without backhaul delay. However, a different user association strategy should be applied to achieve optimal energy consumption, which is: u_1, u_2 and u_3 associate with b_1 , others associate with b_2 . In this case, users associate with their nearest SBSs. Under practical scenarios, the tradeoff relationship between energy consumption and end-to-end file delivery delay is more complicated. In this paper, for the first time, we study such kind of tradeoff in cache-enabled DSCNs. The main contributions are described as follows.

1) In cache-enabled DSCNs, we analyze end-to-end file delivery delay and energy consumption. Based on our analysis, we formulate the energy-delay tradeoff problem as a mixed integer programming (MIP) problem, where file placement, user association and power control are jointly considered.

2) To alleviate traffic pressure on the backhaul, file placement is performed during off-peak time. Based on this fact, we propose a local popular file placement policy at each SBS. In the proposed policy, the optimal file placement problem is converted to a knapsack problem and solved by an efficient greedy algorithm.

3) With the proposed file placement policy, the energy-delay tradeoff problem is reduced to a mixed integer linear programming (MILP) problem and is further decomposed with Benders decomposition method. Then, an efficient algorithm is proposed to approach the optimal association and power solution by iteratively shrinking the gap of the upper and lower bounds.

Extension simulations are carried out to validate our the-

TABLE I: NOTATIONS

Symbol	Description
b_j, u_i, f_k	SBS, user and file indexed by j, i, k respectively
p_j, e_j	Transmission power and energy consumption at b_j
C_j	Cache capacity of b_j
τ_k	Wireless transmission delay of f_k
ρ_{ik}	u_i 's preference for f_k
ψ_{jk}	Popularity of f_k at b_j
d_{ij}^k	File delivery delay for f_k when u_i associates with b_j
$\theta_{ik} \in \{0, 1\}$	If u_i requests f_k , $\theta_{ik} = 1$.
$x_{ij} \in \{0, 1\}$	If u_i associates with b_j , $x_{ij} = 1$.
$y_{ik} \in \{0, 1\}$	If f_k is in cache of b_j , $y_{ik} = 1$.

oretical and algorithmic work. The results demonstrate that the proposed algorithms have fast convergence speed and can achieve the desired tradeoff between energy consumption and end-to-end file delivery delay.

The rest of the paper is organized as follows. Section II gives an overview of the system model. The energy-delay tradeoff problem is formulated in cache-enabled DSCNs in Section III. In Section IV, a local popular file placement policy is proposed. Then, the energy-delay tradeoff problem is decomposed and solved based on Benders' decomposition method. Performance evaluation is presented in Section V. Finally, we conclude the paper in Section VI.

II. SYSTEM MODEL

Consider a downlink DSCN consisting of B SBSs (i.e., femto base stations or pico base stations) indexed by a set $\mathcal{B} = \{1, 2, \dots, B\}$, as shown in Fig. 1. All SBSs are cache-enabled and the cache capacity of SBS b_j is denoted by C_j ($j \in \mathcal{B}$). U users are randomly deployed in the coverage of DSCNs. Let \mathcal{U} denote the user index set and $\mathcal{U} = \{1, 2, \dots, U\}$. Assume each user u_i ($i \in \mathcal{U}$) can only associate with one SBS.

The requested files are indexed by a set $\mathcal{F} = \{1, 2, \dots, F\}$, which are stored as a file library at the file server and cached at SBSs according to file placement policies. For file f_k ($k \in \mathcal{F}$), its size is denoted by s_k and its QoS requirement in terms of rate denoted by R_k . It means that the transmission rate of f_k should be not less than R_k . SBS b_j employs power p_j to transmit files and satisfy their rate requirements.

Some major notations are summarized in Table I.

A. Interference Model

Orthogonal frequency division multiplexing (OFDM) is assumed to be used in cache-enabled DSCNs. In each small cell, resource blocks (i.e., time and frequency) allocated to different users are orthogonal. Therefore, only inter-cell interference from neighbouring cells on the same frequency is considered.

For user u_i associating with SBS b_j , inter-cell interference is $\sum_{l \in \mathcal{B}, l \neq j} p_l g_{il}$, where p_l is the transmission power of SBS b_l and g_{il} denotes the channel gain between u_i and b_l . Thus, signal-interference-noise-ratio (SINR) at u_i associating with b_j can be expressed as

$$\gamma_{ij} = \frac{p_j g_{ij}}{\sum_{l \in \mathcal{B}, l \neq j} p_l g_{il} + \sigma^2},$$

where σ^2 denotes the noise power level. The downlink data rate (bit/s) of u_i is

$$r_{ij} = W \log_2(1 + \gamma_{ij}), \quad (1)$$

where W is the bandwidth allocated to one user. In this paper, we consider practical scenarios where files (e.g., video files) have diverse qualities of service requirements. When u_i requests file f_k , r_{ij} must satisfy $r_{ij} \geq R_k$ to guarantee the delivery quality.

B. Local File Popularity Distribution

In Figure. 1, each SBS is equipped with cache. Files are placed in cache according to the file popularity distribution. Usually, the global file popularity distribution (e.g. Zipf distribution) is used and according to popularity rankings the each SBS will cache the same files [3] [5]. However, such coarse-grained file placement policy ignores the local file popularity characteristic of each small cell, which incurs the waste of cache resource. Local popularity means that different sociological and cultural backgrounds of users at different locations and popularities vary from region to region. Related researches and studies have shown that files or contents have a local popularity characteristic. In [15] [16], authors studied the file popularity distribution and users access patterns in video traffic from a campus network. By analysis of real-world trace data, some significant conclusions are made as follows: 1) global file popularity can not reflect the local file popularity (e.g. a file popularity in a cell site), so the file popularity among different cell sites may be different from each other. 2) users may have strong personal preferences toward their specific file categories.

It is reasonable to assume that during T , the popularity distribution of the files and the user preference for the files are fixed. Typical examples include popular news and short videos, which are updated every 1-3 hours. Besides, another important assumption is made that during the same time scale T , the users in the covering area of each cell are fixed. That is to say, the users move slowly within the covering of the cell during T . Therefore, for the convenience of this research and considering the slow change of the file popularity, we first intend to consider the fixed file popularity of one T .

Based on the above assumptions, to obtain a local file popularity distribution, each SBS first needs to estimate the preference of the central-zone users during off-peak time and then calculates the local file popularity based on the user preference. In a small cell with SBS b_j , based on users' distance to b_j , users are divided into central-zone users and edge users. Central-zone users are just around b_j and are more likely to associates with b_j than edge users from the perspective of energy consumption. Considering SBS b_j , the users index set in the central covering area is denoted by $\Phi_j = \{i \mid u_i \text{ is in the central zone of Cell } b_j\}$. For user preference, we adopt the definition and model of the user preference similar to that in [16], where the user preference is modeled by kernel function. Kernel function can efficiently reflect the correlation between the user and the file. Let ψ_{jk} denotes the popularity of file

f_k at SBS b_j , which is the weighted sum of probabilities that central-zone users request the file f_k . Then we can get the local file popularity distribution at SBS b_j :

$$\psi_{jk} = \sum_{i \in \Phi_j} p(u_i) \rho_{ik}, \quad f_k \in \mathcal{F} \quad (2)$$

where $p(u_i)$ is the probability that user u_i generates a file request. ρ_{ik} is used to stand for u_i 's preference for file f_k . ψ_{jk} denotes the local popularity at b_j and also reflects the ratio of the requests for f_k to the total ones in the central-zone of the small cell at any moment.

III. PROBLEM FORMULATION

In this paper, we attempt to optimize end-to-end file delivery delay and energy consumption by joint power control, user association and file placement. Firstly, we analyze end-to-end file delivery delay and energy consumption of SBSs in cache-enabled DSCNs, respectively. Then, based on our analysis, we formulate the optimization problem as an MILP problem. In this section, end-to-end file delivery delay and system energy consumption in cache-enabled DSCNs are analyzed. Based on our analysis, we formulate the energy-delay optimization problem.

A. Delay and Energy Consumption Analysis

In cache-enabled DSCNs, each SBS is equipped with cache. If SBS caches the file that a user requests, the end-to-end file delivery delay for this user equals to wireless transmission delay. Otherwise, the end-to-end file has to be delivered by the remote file server, and additional backhaul delay is involved. Let d_{ij}^k denote the end-to-end file delivery delay when user u_i associating with SBS b_j requests file f_k . We have

$$d_{ij}^k = \begin{cases} \tau_{ij}^k, & y_{jk} = 1, \\ \tau_{ij}^k + w_j^{BH}, & y_{jk} = 0, \end{cases} \quad (3)$$

where binary variable y_{jk} indicates whether file f_k is cached in b_j or not, and $\tau_{ij}^k = \frac{s_k}{r_{ij}}$ represents wireless transmission delay of f_k transmitted from b_j to u_i . Backhaul delay of b_j is denoted by w_j^{BH} . For wired backhaul, backhaul delay of SBSs is related to the average link distance, the average traffic load and the average number of SBSs connecting to a remote file server in Internet core. Hence, backhaul delay w_j^{BH} at SBS b_j can be modeled to be an exponentially distributed random variable with a mean value of D_j [17].

Here the user request model is given and it is assumed that each user request only one file once time. Let $\theta_{ik} = 1$ denote whether user u_i requests file f_k or not. $\theta_{ik} = 1$ when the u_i requests f_k . Otherwise, $\theta_{ik} = 0$. And $\sum_k \theta_{ik} = 1$ makes u_i only request one file once time. Then, we can derive end-to-end file delivery delay for u_i as follows.

$$d_i = \sum_{j \in \mathcal{B}} \sum_{k \in \mathcal{F}} \theta_{ik} x_{ij} (\tau_{ij}^k + (1 - y_{jk}) w_j^{BH}), \quad (4)$$

where $x_{ij} \in \{0, 1\}$ is a binary variable. If user u_i associates with SBS b_j , $x_{ij} = 1$. Otherwise, $x_{ij} = 0$. Then, one of our

optimization objectives is to minimize end-to-end file delivery delay of all users:

$$\min_{\mathbf{X}, \mathbf{p}, \mathbf{Y}} \sum_{i \in \mathcal{U}} d_i$$

Energy consumption at SBS b_j is expressed as follows:

$$e_j = p_j T_j,$$

where file serving time $T_j = \sum_{i \in \mathcal{U}} \sum_{k \in \mathcal{F}} \theta_{ik} x_{ij} \tau_{ij}^k$ at SBS b_j denotes the time required to complete transmission of all requested files at b_j .

Then, the other objective is to minimize total transmission energy consumption:

$$\min_{\mathbf{X}, \mathbf{p}} \sum_{i \in \mathcal{U}} e_j,$$

B. Energy and Delay Optimization

Compared with optimizing the two objectives separately, jointly optimizing energy and delay belongs to a kind of multi-objective optimization problem. To express such optimization problem, we employ a weighted sum based utility function, which is modeled by the weighted sum of energy cost and delay cost [18]. We can formulate the energy-delay optimization problem as follows.

$$\min_{\mathbf{X}, \mathbf{p}, \mathbf{Y}} \alpha \sum_{j \in \mathcal{B}} e_j + (1 - \alpha) \sum_{i \in \mathcal{U}} d_i \quad (5)$$

$$\text{s.t. } 0 < \sum_{i \in \mathcal{U}} p_j x_{ij} \leq P_j^{\max}, \forall j \in \mathcal{B}, \quad (6)$$

$$r_{ij} \geq R_k, \forall i \in \mathcal{U}, k \in \mathcal{F}, \quad (7)$$

$$x_{ij} \in \{0, 1\}, \forall i \in \mathcal{U}, j \in \mathcal{B}, \quad (8)$$

$$d_i = \sum_{j \in \mathcal{B}} \sum_{k \in \mathcal{F}} \theta_{ik} x_{ij} (\tau_k + (1 - y_{jk}) w_j^{BH}), \quad (9)$$

$$\sum_{j \in \mathcal{B}} x_{ij} = 1, \forall i \in \mathcal{U}, \quad (10)$$

where $\alpha \in [0, 1]$ is reasonable in our paper and indicates the different significance between energy consumption and end-to-end file delivery delay. A larger α means that network operators will pay more attention to reducing energy consumption at the expense of increasing end-to-end file delivery delay. Constraint (6) makes sure that total power supply does not exceed maximal power available at each SBS. Constraint (7) represents the transmission rate requirements of each file. Specifically, the extended expression of constraint (7) is

$$W \log \left(1 + \frac{p_j g_{ij}}{\sum_{l \in \mathcal{B}, l \neq j} p_l g_{il} + \sigma^2} \right) \geq W \log (1 + x_{ij} \gamma_k \theta_{ik}), \quad (11)$$

where γ_k is SINR threshold that satisfies the rate requirement of file f_k . Constraint (7) can be rewritten as $\frac{p_j g_{ij}}{\sum_{l \in \mathcal{B}, l \neq j} p_l g_{il} + \sigma^2} \geq x_{ij} \gamma_k \theta_{ik}$. Thus, in stead of R_k , γ_k can be used to represent the file transmission requirement. Each user association decision is indicated by a binary variable x_{ij} and each user can only associates with one SBS, which are expressed as constraint (8) and (10).

The problem (5) with discrete user association decision and continuous power control is an MIP problem. In order to solve the problem, file placement, user association and power control should be jointly considered, which also makes the problem much more complicated.

To further clarify the complexity of the problem (5), we introduce a simple optimization instance. By the analysis of such instance, we show the challenge of solving (5) and the proposition 1 is given below:

Proposition 1. *When a file placement policy is chosen, for any feasible power allocation result, the problem (5) is NP-hard.*

Proof. In order to prove the proposition, we first introduce the well-known Multidimensional 0-1 Knapsack Problems(MKP) with block angular structures which is a NP-Hard problem [19] [20].

In the problem MKP, there are q knapsacks with a maximum weight load denoted by $(w_j, j = 1, \dots, q)$. And there are n items. Each item has different values and weights in different knapsacks. Then the value and weight vectors of items in each knapsack can be denoted by $(\mathbf{v}_j, j = 1, \dots, q)$ and $(\mathbf{b}_j, j = 1, \dots, q)$, respectively. The MKP policy $(\mathbf{x}_j \in \{0, 1\}^n, j = 1, \dots, q)$ is to let each knapsack to select a subset of items, such that the total value of all knapsacks is maximized under limited weight load of each knapsack. The formulation os MKP is

$$\begin{aligned} & \max_{\mathbf{x}_1, \dots, \mathbf{x}_q} \mathbf{v}_1^T \mathbf{x}_1 + \dots + \mathbf{v}_q^T \mathbf{x}_q \\ & \text{s.t. } \begin{cases} \mathbf{M}_1 \mathbf{x}_1 + \dots + \mathbf{M}_q \mathbf{x}_q \preceq \mathbf{a}_0 \\ \mathbf{b}_1^T \mathbf{x}_1 \leq w_1 \\ \vdots \\ \mathbf{b}_q^T \mathbf{x}_q \leq w_q \\ \mathbf{x}_j \in \{0, 1\}^n, j = 1, \dots, q, \end{cases} \end{aligned}$$

where \mathbf{v}_j and \mathbf{x}_j are n dimensional value column vectors, $\mathbf{M}_j, j = 1, \dots, q$ are $m_0 \times n$ coefficient matrices, and the first set of inequalities denotes m_0 coupling constraints. The constraint $\mathbf{b}_j^T \mathbf{x}_j \leq w_j$ are m_j dimensional block constraints, where \mathbf{b}_j are n dimensional weight column vectors. Then such problem can be viewed as a multidimensional 0-1 knapsack problem with a block angular structure.

Back to problem (5), a simple optimization instance is introduced. When the file placement and power allocation result are given, (5) becomes a simple user association problem. Let $(\hat{p}_j, j \in \mathcal{B})$ and $(\hat{y}_{jk}, j \in \mathcal{B}, k \in \mathcal{F})$ denote the file placement and power allocation results. Specifically, when user u_i is connected to SBS b_j , the related energy consumption and end-to-end file delivery delay are $\hat{e}_{ij} = \hat{p}_j \sum_{k \in \mathcal{F}} \theta_{ik} \tau_{ij}^k$ and $\hat{d}_{ij} = \sum_{k \in \mathcal{F}} \theta_{ik} (\tau_{ij}^k + (1 - \hat{y}_{jk}) w_j^{BH})$, respectively. According to (1), for the given $(\hat{p}_j, j \in \mathcal{B})$ the data rate r_{ij} and τ_{ij}^k are fixed. Thus, \hat{e}_{ij} is a fixed value. Besides, as file placement policy $(\hat{y}_{jk}, j \in \mathcal{B}, k \in \mathcal{F})$ is known, according to (4), \hat{d}_{ij} becomes a known end-to-end file delivery delay. Let cost coefficient $c_{ij} = \hat{e}_{ij} + \hat{d}_{ij}$ to denote the sum of \hat{e}_{ij} and \hat{d}_{ij} . Base on the above analysis, we can rewrite our problem

(5) and obtain the below problem. To make the formulation more explicit, we intend to maximize the negative value of our problem.

$$\begin{aligned} \max_{\mathbf{X}} \quad & - \sum_{i \in \mathcal{U}} \sum_{j \in \mathcal{B}} (c_{ij} x_{ij}) \\ \text{s.t.} \quad & \begin{cases} 0 < \sum_{i \in \mathcal{U}} \hat{p}_j x_{ij} \leq P_j^{max}, \forall j \in \mathcal{B} \\ \sum_{j \in \mathcal{B}} x_{ij} = 1, \forall i \in \mathcal{U}, \\ x_{ij} \in \{0, 1\}, \forall i \in \mathcal{U}, j \in \mathcal{B}, \end{cases} \end{aligned} \quad (12)$$

After comparing the problem (12) and the formulation of MKP, it is apparent that (12) is equivalent to the original instance of MKP. Therefore, the problem (12) is NP-Hard. \square

IV. PROBLEM SOLUTION

The problem (5) is difficult to be solved directly due to the coupling relationship among file placement, user association and power control. Then, we solve the problem in two stages, i.e. caching stage and delivery stage, based on the observation that caching is performed during off-peak time. At the caching stage, a local popular file placement policy is proposed by estimating user preference at each SBS. At the delivery stage, with given caching status at SBSs, the MIP problem is further decomposed by Benders' decomposition method.

A. Local Popular File Placement Policy

File processing consists of two stages, i.e., file caching and file delivery, which are implemented in different time scales. Different from the file delivery phase including the procedures of user association and power control, file caching is determined at a much slower time-scale. In file caching stage, based on the file popularity, files are often pre-fetched from the file server and proactively cached at SBSs during off-peak periods to alleviate traffic pressure on the backhaul link [21]. In some researches [2] [22] [23], authors studied the mixed-timescale problem: long-timescale file placement policy and the short-term user association and wireless resource allocation. However, in [23], each BS has to cache the same files when they adopt the global file popularity-aware caching policy, which ignores the difference of the file popularity among small cells.

In this paper, compared with the short-term user association and power control, the file placement policy is implemented during a longer periods T such as some minutes or hours. During T , the popularity distribution of the files and the user preference for the files are fixed. For the convenience of this research and to avoid considering the tumultuous changes of the file popularity, the fixed file popularity of one T is considered.

Based on the above analysis, we propose a local popular file placement policy. With the goal of maximizing the cache hit ratio, the local most popular files should be cached by each SBS during off-peak time. At a SBS, the local file popularity distribution can be obtained according to (2). Thus, the optimal file placement problem can be solved independently for each

SBS. Considering SBS b_j , we can convert the optimal file placement problem to a knapsack problem, which is expressed as follows.

$$\begin{aligned} \max_{\mathbf{y}_j} \quad & \psi_j = \sum_{k \in F} \psi_{jk} y_{jk} \\ \text{s.t.} \quad & \sum_{k \in F} s_k y_{jk} \leq C_j, \forall j \in \mathcal{B} \\ & y_{jk} \in \{0, 1\}, \end{aligned} \quad (13)$$

where the binary variable y_{jk} denotes the caching decision at b_j . As the knapsack problem is NP-Hard, a heuristic greedy algorithm for maximizing the caching hit probability is proposed and described as Algorithm 1.

Algorithm 1: Greedy Algorithm for Maximum Caching hit Probability

Input: \mathcal{F} , B , $\psi_{jk}, \forall k \in \mathcal{F}$.
Output: ψ_j^* , $\mathbf{y}_j^*, \forall j \in \mathcal{B}$.

- 1 **repeat**
- 2 $j = 1$;
- 3 Sort \mathcal{F} into \mathcal{F}_j^\diamond in descending order of $\frac{\psi_{jk}}{s_k}$;
- 4 Set $g \leftarrow 0$, $k \leftarrow 1$, and $y_{jk}^\diamond \leftarrow 0, \forall k \in \mathcal{F}$;
- 5 **repeat**
- 6 Let f'_k be the k -th element of \mathcal{F}_j^\diamond ;
- 7 Set $y_{j f'_k}^\diamond \leftarrow 1$;
- 8 Update $g \leftarrow g + s_k$ and $k = k + 1$;
- 9 **until** $g > C_j$ and $k > F$;
- 10 Calculate ψ_j by (13) using ψ_j ;
- 11 $j = j + 1$;
- 12 **until** $j > B$;

The algorithm requires B iterations. The complexity of each iteration is $\mathcal{O}(C_j \log C_j)$.

B. Association and Power Solution

With the proposed popular file placement policy, the remaining problem (5) is reduced to a MILP problem but still complicated with coupled user association and power control. To solve the MILP problem, Benders' decomposition is used to partition it into two small problems and obtain a ϵ -optimal solution by iterations.

1) *Motivation:* To reduce the complexity of the problem (5), wireless transmission delay τ_{ij}^k in (3) is relaxed to $\frac{s_k}{R_k}$. Then total wireless file transmission time $\sum_{i=1}^U \sum_{j=1}^B \sum_{k=1}^F \theta_{ik} \tau_{ik} x_{ij}$ becomes a constant D . This is because that for user u_i , $\sum_{k=1}^F \theta_{ik} = 1$ and $\sum_{j=1}^B x_{ij} = 1$ hold. Thus, the system load among SBSs can be controlled by a load coefficient β_j based on the capability of SBS $b_j (j \in \mathcal{B})$. And the load of SBS b_j is can be expressed as $T_j = D \cdot \beta_j = \beta_j \sum_{i=1}^U \sum_{k=1}^F \theta_{ik} \tau_{ik} x_{ij}$.

With the above assumption and observation, given the proposed local popular file placement policy, the problem (5) becomes an MILP problem. However, user association and

power control is still coupled both in the objective function and the constraints, which make the problem complicated to be solved. Fortunately, based on the characteristics of our problem, the Benders' decomposition can be adopted to decomposition it.

Benders' decomposition is proposed for a class of MILP problems [24] [25]. Instead of thinking about all variables of a problem, it first consider the continuous part. Thus, the original optimization problem is partitioned into two smaller problems: a subproblem with only continuous variables and a master problem with one continuous variable and multiple integer variables. To be specific, when integer variables are fixed, the resulting problem (subproblem) becomes a continuous linear program (LP) problem which can be solved by the standard duality theory of convex optimization. And then, the results of the dual problem can be transferred to the master problem.

2) *Subproblem*: According to the Benders' decomposition method, after the $(t-1)$ th iteration, the energy consumption problem is formulated as a subproblem:

$$\min_{\mathbf{p}} \sum_{j \in \mathcal{B}} e_j \quad (14)$$

$$\text{s.t. } 0 < \sum_{j \in \mathcal{B}} x_{ij}^{(t-1)} p_j \leq P_j^{max}, \forall j \in \mathcal{B}, \quad (15)$$

$$\frac{g_{ij} p_j + \varrho^{-1} (1 - x_{ij}^{(t-1)})}{\sum_{l \in \mathcal{B}, l \neq j} p_l g_{il} + \sigma^2} \geq \gamma_k \theta_{ik}, \forall i \in \mathcal{B}, j \in \mathcal{U}. \quad (16)$$

Given the user association strategy, the power constraint is convex and hence will not change the nature of the formulated problem. To satisfy the standard problem form in Benders' decomposition, we use a equivalent transformation technique. A parameter ϱ is introduced satisfying $\varrho = \min_i \frac{1}{\gamma_{fi} ((I-1)\bar{p}\bar{g} + \sigma^2)}$ where $\bar{p} = \max_j \{P_j^{max}\}$ and $\bar{g} = \max_{i,j} \{g_{ij}\}$. The introduction of ϱ will not change the optimal solution to the problem (5). For $x_{ij}^* = 1$, the formulation forms of (11) and (7) are equivalent. For $x_{ij}^* = 0$, from (7) we can deduce

$$\frac{g_{ij} p_j + \varrho^{-1}}{\sum_{l \neq j} g_{il} p_l + \sigma^2} \geq \frac{((I-1)\bar{p}\bar{g} + \sigma^2) \gamma_{fk} \theta_{ik}}{\sum_{l \neq j} g_{il} p_l + \sigma^2} \geq \gamma_{fi}, \quad (17)$$

No matter what p_{ij}^* is, (17) always holds. In order to optimize energy consumption, the objective will make p_{ij}^* be 0. And then based on the duality theory [26], we can get the dual

function of (14) as follows:

$$\begin{aligned} \max_{\boldsymbol{\mu}, \boldsymbol{\nu}} \quad & h(\mathbf{X}^{(t-1)}, \boldsymbol{\mu}, \boldsymbol{\nu}) \\ \text{s.t.} \quad & h(\mathbf{X}^{(t-1)}, \boldsymbol{\mu}, \boldsymbol{\nu}) \\ & = \sum_{j \in \mathcal{B}} (-P_j^{max} \mu_j) + \sum_{i \in \mathcal{U}} \sum_{j \in \mathcal{B}} (\varrho^{-1} (x_{ij}^{(t-1)} - 1) + \sigma^2 \gamma_{fi}) \nu_{ij}, \\ & e_j + \mu_j + \sum_{i \in \mathcal{U}} [-g_{ij} \nu_{ij} + \sum_{l \in \mathcal{B}, l \neq j} (\gamma_l \theta_{il} g_{ij} \nu_{il})] \geq 0, \forall j \in \mathcal{B}, \\ & \boldsymbol{\mu} = [\mu_j] \succeq 0, \forall j \in \mathcal{B}, \\ & \boldsymbol{\nu} = [\nu_{ij}] \succeq 0, \forall j \in \mathcal{B}, i \in \mathcal{U}. \end{aligned} \quad (18)$$

The dual function (18) is an LP problem, so Interior Point Method can be used to obtain the optimal solution [27].

3) *Master Problem*: In the remaining problem, we mainly focus on end-to-end file delivery delay and low bound of energy consumption denoted by η , both of them depend on user association \mathbf{X} .

$$\begin{aligned} \min_{\eta, \mathbf{X}} \quad & \alpha \eta + (1 - \alpha) \sum_{i \in \mathcal{U}} \sum_{j \in \mathcal{B}} \sum_{k \in \mathcal{F}} \theta_{ik} d_{ij}^k x_{ij} \\ \text{s.t.} \quad & h(\mathbf{X}, \boldsymbol{\mu}_p^{(m)}, \boldsymbol{\nu}_p^{(m)}) \leq \eta, \forall m = 1, \dots, k_1, \\ & h(\mathbf{X}, \boldsymbol{\mu}_q^{(n)}, \boldsymbol{\nu}_q^{(n)}) \leq 0, \forall n = 1, \dots, k_2, \\ & x_{ij} \in \{0, 1\}, \forall i \in \mathcal{U}, j \in \mathcal{B}, \\ & \sum_{j=1}^B x_{ij} = 1, \forall i \in \mathcal{U}, \end{aligned} \quad (19)$$

where in the optimal cut $h(\mathbf{X}, \boldsymbol{\mu}_p^{(m)}, \boldsymbol{\nu}_p^{(m)}) \leq \eta$, $(\boldsymbol{\mu}_p^{(m)}, \boldsymbol{\nu}_p^{(m)})$ is the optimal solution of the bounded problem (18). And in the feasible cut $h(\mathbf{X}, \boldsymbol{\mu}_q^{(n)}, \boldsymbol{\nu}_q^{(n)}) \leq 0$ $(\boldsymbol{\mu}_q^{(n)}, \boldsymbol{\nu}_q^{(n)})$ is the unbounded direction of the unbounded problem (18). Both $(\boldsymbol{\mu}_p^{(m)}, \boldsymbol{\nu}_p^{(m)})$ and $(\boldsymbol{\mu}_q^{(n)}, \boldsymbol{\nu}_q^{(n)})$ form the constraint set of the problem (19). At t th iteration, k_1 and k_2 must satisfy: $k_1 + k_2 = t$.

4) *Upper and Lower Bounds*: The solutions of the problem (18) and (19) at each iteration provide the upper and lower bounds of the optimal values respectively. Proposition 2 as follows: (UB and LB are denoted by $\Psi_U^{(t)}$ and $\Psi_L^{(t)}$)

Proposition 2. *At each iteration, the upper bounds $\Psi_U^{(t)}$ and lower bounds $\Psi_L^{(t)}$ are updated as follows: $\Psi_L^{(t)} = N^{(t)}$, and $\Psi_U^{(t)} = \min_{0 \leq r \leq t-1} \{M^{(r)} + \rho \sum_i \sum_j \sum_k \theta_{ik} d_{ij}^k x_{ij}^{(r)}\}$, where $M^{(t)}$ and $N^{(t)}$ are the optimal values of (18) and (19) at the t th iteration, respectively.*

Proof. Lower Bound:

First, we consider how to calculate lower bound $\Psi_L^{(t)}$ of the original problem (5) at t -th iteration. The problem (18) is a dual function of the linear function (14). According to the strong duality of LP, we can say that the problem (5) is equivalent to that in (20):

$$\min_{\mathbf{X}, \boldsymbol{\mu}, \boldsymbol{\nu}} \alpha h(\mathbf{X}, \boldsymbol{\mu}, \boldsymbol{\nu}) + (1 - \alpha) \sum_{i \in \mathcal{U}} \sum_{j \in \mathcal{B}} \sum_{k \in \mathcal{F}} \theta_{ik} d_{ij}^k x_{ij} \quad (20)$$

$$\text{s.t. } x_{ij} \in \{0, 1\}, \forall i \in \mathcal{U}, j \in \mathcal{B}, \quad (21)$$

$$\sum_{j=1}^B x_{ij} = 1, \forall i \in \mathcal{U}. \quad (22)$$

Compared (19) and (20), the relaxing constraints in (19) makes (19) is a relaxation of (20). At each iteration, a new constraint is added to the problem (19). That is, the constraint set in the problem (19) will be updated after each iteration. According to the duality theory, this update of constraint set makes $(N^{(t)} = \alpha \eta^{(t)} + (1 - \alpha) \sum_i \sum_j \theta_{ik} d_{ij}^k x_{ij}^{(t)})$ become lower bound of the optimal value in (20).

Then, $N^{(t)}$ is also the lower bound of the optimal values $\alpha \sum_j p_j^* \tau_j + (1 - \alpha) \sum_i \sum_j \theta_{ik} d_{ij}^k x_{ij}^*$, where $(\mathbf{X}^*, \mathbf{P}^*)$ is assumed to be the optimal solution of the problem (5).

Therefore, the optimal value $N^{(t)}$ of (19) at t -th iteration is a lower bound $\Psi_U^{(t)}$ of problem (5).

Upper Bound:

We prove that $\min_{0 \leq r \leq t-1} \{\alpha M^{(r)} + (1 - \alpha) \sum_i \sum_j \theta_{ik} d_{ij}^k x_{(ij)}^{(r)}\}$ is the upper bound of the problem (5) at the t -th iteration of .

As $\mathbf{y}^{(t-1)}$ makes the problem (18) either bound or unbound, the optimal value $M^{(r)}$ of (18) will be either finite or infinite, respectively. If $M^{(r)}$ is infinite, it is apparent that $\min_{0 \leq r \leq t-1} \{\alpha M^{(r)} + (1 - \alpha) \sum_i \sum_j \sum_k \theta_{ik} d_{ij}^k x_{(ij)}^{(r)}\}$ is the upper bound. If $M^{(r)}$ is finite, $\omega = \arg \min_{0 \leq r \leq t-1} \{\alpha M^{(r)} + (1 - \alpha) \sum_i \sum_j \theta_{ik} d_{ij}^k x_{(ij)}^{(r)}\}$, where $0 \leq \omega \leq t - 1$. Correspondingly, $(\mathbf{X}^{(\omega)}, \boldsymbol{\mu}^{(\omega)}, \boldsymbol{\nu}^{(\omega)})$ and power $\mathbf{p}^{(\omega)}$ are the optimal solution of $h(\mathbf{X}, \boldsymbol{\mu}, \boldsymbol{\nu})$ and (14). According to the strong duality, we have $M^{(\omega)} = h(\mathbf{X}^{(\omega)}, \boldsymbol{\mu}^{(\omega)}, \boldsymbol{\nu}^{(\omega)}) = \sum_{i=1}^U \sum_{j=1}^B p_j^{(\omega)} \tau_j$. If we

assume $\alpha \sum_{j=1}^B p_j^{(\omega)} \tau_j + (1 - \alpha) \sum_{i=1}^U \sum_{j=1}^B \theta_{ik} d_{ij}^k x_{ij}^{(\omega)}$ is less than

$\alpha \sum_{j=1}^B p_j^{(*)} + (1 - \alpha) \sum_{i=1}^U \sum_{j=1}^B \theta_{ik} d_{ij}^k x_{ij}^*$, then $(\mathbf{P}^{(\omega)}, \mathbf{X}^{(\omega)})$ will be the optimal solution of the problem (5). It means after ω th iteration $\Psi_U^{(\omega)} < \Psi_L^{(\omega)}$, which is contradictory. Hence, $\min_{0 \leq r \leq t} \{\alpha M^{(r)} + (1 - \alpha) \sum_i \sum_j \sum_k \theta_{ik} d_{ij}^k x_{(ij)}^{(r)}\}$ is the upper bound $\Psi_U^{(t)}$ of the problem (5). \square

5) *Relaxed Master Problem (RMP)*: Considering the binary nature of x_{ij} , which domains the computation complexity of the problem (5), we decide to use a linear relaxation method. Firstly, instead of $x_{ij} \in \{0, 1\}$, we make $x_{ij} \in [0, 1]$ by Proposition 3. Then we construct an equivalent formulation with a penalty function by Proposition 4, which can reduce the computation complexity of the problem (5).

In Proposition 3, the equivalence relationship between the binary constraint and the linear relaxation is elaborated.

Proposition 3. *Given the definitions*

$$A := [0, 1]^{UB}, \quad (23a)$$

$$B := \left\{ \mathbf{x} \in R^{UB} : \sum_{i \in \mathcal{U}} \sum_{j \in \mathcal{B}} x_{ij}^2 - \sum_{i \in \mathcal{U}} \sum_{j \in \mathcal{B}} x_{ij} < 0 \right\}, \quad (23b)$$

the binary set $\{0, 1\}^{UB}$ is the difference of two convex sets A and B , i.e., $\{0, 1\}^{UB} = A \setminus B$.

Proof. Obviously, we can get $\{0, 1\}^{UB} \subset A \setminus B$. Besides, $x_{ij} \in \{0, 1\}^{UB}$ is the result of

$$x_{ij} - x_{ij}^2 = 0, \quad i = 1, \dots, U; j = 1, \dots, B. \quad (24)$$

Then, $x_{ij} - x_{ij}^2 \geq 0$ holds for each $x_{ij} \in A$ and $\sum_{i=1}^U \sum_{j=1}^B x_{ij} - \sum_{i=1}^U \sum_{j=1}^B x_{ij}^2 \leq 0$ for $x_{ij} \notin B$, so each $x_{ij} \in A \setminus B$ makes $x_{ij} - x_{ij}^2 = 0$. Therefore $x_{ij} \in A \setminus B$ is feasible to (24), i.e., $A \setminus B \subset \{0, 1\}^{UB}$. \square

Based on Proposition 3, (19) can be equivalently transformed to (25). The detailed proof is given in Proposition 4.

Proposition 4. *We can relax the binary set \mathbf{X} in (19) to $[0, 1]^{UB}$ and obtain an new objective function (25) which is equivalent to (19) when $\lambda \gg 1$.*

RMP:

$$\begin{aligned} \min_{\eta, \mathbf{X}} \quad & \alpha \eta + (1 - \alpha) \sum_{i \in \mathcal{U}} \sum_{j \in \mathcal{B}} \sum_{k \in \mathcal{F}} \theta_{ik} d_{ij}^k x_{ij} \\ & + \lambda \sum_{i=1}^U \sum_{j=1}^B (x_{ij} - x_{ij}^2) \end{aligned} \quad (25)$$

$$\begin{aligned} \text{s.t.} \quad & h(\mathbf{X}, \boldsymbol{\mu}_p^{(m)}, \boldsymbol{\nu}_p^{(m)}) \leq \eta, \forall m = 1, \dots, t_1, \\ & h(\mathbf{X}, \boldsymbol{\mu}_q^{(n)}, \boldsymbol{\nu}_q^{(n)}) \leq 0, \forall n = 1, \dots, t_2, \\ & x_{ij} \in [0, 1], \forall i \in \mathcal{U}, j \in \mathcal{B}, \\ & \sum_{ij} x_{ij} = 1, \forall j \in \mathcal{B}, \end{aligned}$$

where λ is a constant penalty factor. The large parameter λ makes the relaxed \mathbf{X} be as binary as possible.

Proof. See Appendix. \square

Based on Proposition 4, when an appropriate value is chosen for λ , the problem (19) is equivalent to the problem (25) in the sense that they share the same optimal values as well as optimal solution. The RMP is a minimization of a concave quadratic function which can be solved by the method in [28].

C. Algorithm

In order to get an ϵ -optimal value, we propose a user association and power control (UCWT) algorithm in Algorithm 2.

1) *Analysis of the Convergency*: The UCWT algorithm uses the gap between $\Psi_U^{(t)}$ and $\Psi_L^{(t)}$ as the termination criterion. In particular, if the gap is equal to zero the exact global optimal solution to the problem (5). If the gap is equal to ϵ , an ϵ -optimal value is obtained. The following theorem proves the convergence of the proposed algorithm.

Theorem 1. *After a finite number of iterations, the proposed UCWT algorithm converges to a global optimal value of (5).*

Algorithm 2: User assoCiation and poWer conTrol (UCWT) Algorithm for Energy-Delay Tradeoff

Input: P^{max} , γ , θ
Output: P^* , X^*

- 1 **Initialization:** Let $X^{(0)} = \mathbf{0}$, $\Psi_L^{(0)} = -\infty$, $\Psi_U^{(0)} = +\infty$, $t = 1$, $m = 1$, $n = 1$;
 - 2 **repeat**
 - 3 **Subproblem:**
 - 4 Solve $(\mu^{(t)}, \nu^{(t)}) = \arg \max_{(\mu, \nu)} h(X^{(t-1)}, \mu, \nu)$ in (18) with Interior Point Method;
 - 5 **if** (18) is bounded **then**
 - 6 | Get extreme point: $(\mu_p^{(m)}, \nu_p^{(m)}) = (\mu^{(t)}, \nu^{(t)})$;
 - 7 **else**
 - 8 | Get extreme ray: $(\mu_q^{(n)}, \nu_q^{(n)}) = (\mu^{(t)}, \nu^{(t)})$;
 - 9 **end**
 - 10 Calculate upper bound $\Psi_U^{(t)}$ with $\omega = \arg \min_{0 \leq r \leq t-1} \{\alpha M^{(r)} + (1-\alpha) \sum_i \sum_j \theta_{ik} d_{ij}^k x_{ij}^{(r)}\}$;
 - 11 **RMP:**
 - 12 Add a constraint: $h(X, \mu_p^{(m)}, \nu_p^{(m)}) \leq \eta$ or $h(X, \mu_q^{(n)}, \nu_q^{(n)}) \leq 0$ to (25);
 - 13 Solve (25) to obtain $X^{(t)}$;
 - 14 Calculate lower bound with the method in [28]: $\Psi_L^{(t)} = \alpha \eta^{(t)} + (1-\alpha) \sum_{i=1}^U \sum_{j=1}^B \sum_{k=1}^F \theta_{ik} d_{ij}^k x_{ij}^{(t)}$;
 - 15 $t = t + 1, n = n + 1, m = m + 1$;
 - 16 **until** $\Psi_U^{(t-1)} - \Psi_L^{(t-1)} \leq \epsilon$;
 - 17 Get optimal solution P^* through solving the dual problem of (18) with $X^{(\omega)}$. Let optimal solution $X^* = X^{(\omega)}$.
-

Proof. After each iteration, the constraint set of the problem (25) is updated by adding $h(X, \mu_p^{(m)}, \nu_p^{(m)}) \leq \eta$ or $h(X, \mu_q^{(n)}, \nu_q^{(n)}) \leq 0$, where $(\mu^{(m)}, \nu^{(m)})$ or $(\mu^{(n)}, \nu^{(n)})$ is one feasible solution of the subproblem (18). According the linear programming theory, the solution set of the problem (18) is a finite number of the extreme points or extreme rays which determine the total iteration number. After finite iterations, the constraint set of the subproblem (18) is completed by adding the total extreme points or extreme rays of (18). This implies that optimal user association (X^*) can be obtained by (19). As $\Psi_L^{(t)}$ is increasing after each iteration t , the Ψ_L will arrive at the optimal value of problem (5). For $\Psi_U^{(t)}$ is also decreasing after each iteration t , $\Psi_U^{(t)}$ finally satisfies the optimal value of (5) with the optimal solution (X^*) and (P^*) solved by (18). At last, the gap of $\Psi_L^{(t)}$ and $\Psi_U^{(t)}$ is shrunk to 0 within a finite number of iterations. \square

2) *Analysis of the Complexity:* For the subproblem (18), it is an LP problem and Interior Point Method has been proposed as an efficient method in [27]. Here, Interior Point Method needs be executed $\mathcal{O}(U^2 B^2)$ times and at each time the complexity is $\mathcal{O}(U^2 B)$. So the total complexity of subproblem is $\mathcal{O}(U^4 B^3)$.

TABLE II: SIMULATION SETTING

Symbol	Description
Small cell radius	40m
Maximal transmit power of each SBS	23dBm
Number of subchannels	16
Subchannel bandwidth	200KHz
Thermal noise density	-174dBm/Hz
Number of files	600
Size of file	0.5MB to 50MB

For the RMP (25), it is a concave quadratic function which can be solved by the method in [28]. It needs t^2 iterations and each iteration complexity is $\mathcal{O}(U^2 B)$. So the total complexity of RMP is $\mathcal{O}(t^2 U^2 B)$.

According to Theorem 1, the total number of iterations in UCWT, relate to the finite number of extreme points or extreme rays in subproblem (18), is determined by the scale of the problem, i.e., total user number U and total SBS number B . Thus, the total iterations in UCWT will be varied under different value of U and B . In our simulations, UCWT usually obtains a ϵ -optimal value after tens of iterations.

V. PERFORMANCE EVALUATION

Extensive simulations are carried out to validate our work. The results demonstrate the convergency of the proposed algorithm. Moreover, with the proposed algorithm, the desired energy-delay tradeoff can be obtained under various scenarios in cache-enabled DSCNs.

A. Simulation Settings

In the simulations, we study a cache-enabled DSCN consisting of 25 small cells in a 250m-by-250m square area. We assume that SBSs are uniformly distributed over a two-dimensional network layout and each SBS is located at the center of its serving cell. Users are randomly generated and deployed according to the uniform distribution. The radius of the central area is 25 meters [29]. We consider a distance dependent path loss model and the loss factor from SBS b_j to user u_i is given as $d_{ij}^{(-\kappa)}$ ($2 \leq \kappa \leq 5$). The physical layer parameters are based on the 3GPP evaluation methodology document [30]. We use a file library of 600 files, the size of which follows the uniform distribution between [0.5, 50](MB). The SINR requirement of each file is set between 1.5 and 5, which can be converted to rate requirement according to (11). We assume that the probability that each user generates a request is equal, namely $p(u_i) = \frac{1}{|\Phi_j|}$. Therefore, Eq. (2) can be rewritten as: $\psi_{jk} = \sum_{i \in \Phi_j} \frac{1}{|\Phi_j|} \rho_{ik}$, where $|\Phi_j|$ is the cardinality of the set Φ_j . The penalty parameter λ for the proposed algorithm is set to $(10 P^{max} + \sum_{i=1}^B \sum_{k=1}^F \theta_{ik} \tau_k + \sum_{j=1}^B w_j^{BH})$, such that the value of the penalty term $\lambda \sum_{i=1}^U \sum_{j=1}^B (x_{ij} - x_{ij}^2)$ is comparable to the value of (19) [31]. Given that each SBS has the same maximal transmission power, load coefficient β_j defined in Section III-A is set to be $1/B$. Some major parameters are configured in Table II.

In Algorithm 1, each user preference follows normal distribution with different mean value (1~600) and variances over

the total files, which is implemented at the beginning of the simulation. For each SBS, the radius of the center area is set as $25m$. The central user requests for file f_k at SBS b_j must satisfy: $\frac{\sum_{i \in \Phi_j} \theta_{ik}}{|\Phi_j|} = \psi_{jk}$.

B. Convergence Analysis of UCWT

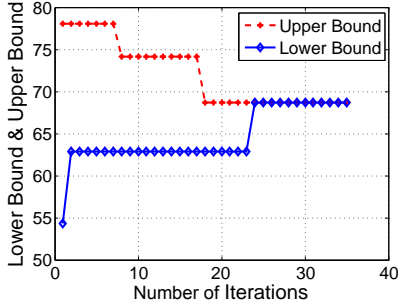


Fig. 2: Upper and the lower bounds when performing UCWT

In order to verify the convergency of the proposed UCWT algorithm, the number of iterations for an optimal value is plotted in Fig. 2. The cache capacity of each SBS follows a normal distribution with mean value(15 files) and the number of users is 150. Total user requests for files in central area of b_j follows the distribution $\psi_{jk}, \forall k \in \mathcal{F}$. From Fig. 2, the upper bound and lower bound become closer with increasing the number of iterations. Through limited number of iterations, the gap between UB and LB converges to a given ϵ . We observe that, if the number of users is not very large, UCWT can converge to an ϵ -optimal value after tens of iterations, which is due to the fact that the number of the extreme points or rays is limited in this case.

C. Energy-delay Tradeoff by Adjusting α

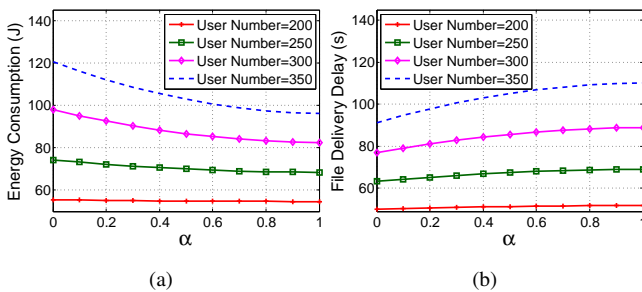


Fig. 3: (a) energy consumption and (b) end-to-end file delivery delay comparison under different number of users by varying α

We investigate the tradeoff characteristics between energy consumption and end-to-end file delivery delay by varying α . Fig. 3 shows the energy-delay tradeoff curves by adjusting α from 0 to 1 given average capacity 15(number of files). We can see that, when the number of users is given, as the α is increasing, energy consumption is in a decreasing trend

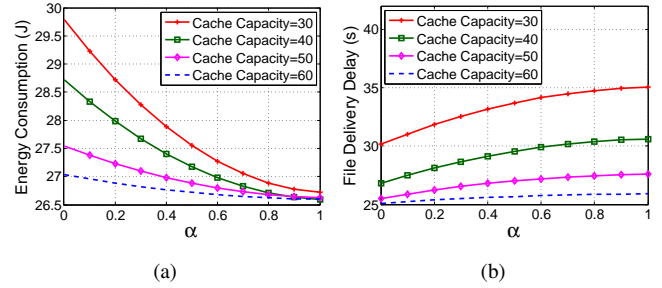


Fig. 4: (a) energy consumption and (b) end-to-end file delivery delay comparison under different average cache capacities by varying α

(Fig. 3(a)) and end-to-end file delivery delay in a increasing trend (Fig. 3(b)). This is because when α increases, more users are forced to associate with the nearer SBSs regardless of their file requests. Thus lower energy consumption is achieved. Besides, by increasing energy consumption by 20%, end-to-end file delivery delay can be reduced by an average 10% with an proper α .

Fig. 4 shows the same tradeoff characteristics between energy consumption and end-to-end file delivery delay under different cache capacities given the number of user 150. Note that, when the average cache capacity is large enough, energy consumption and end-to-end file delivery delay are very small and change a little with various α . This is due to the fact that most of the required files can be cached in the nearest SBSs, which saves a lot energy and delay.

D. Effects of Caching Strategies

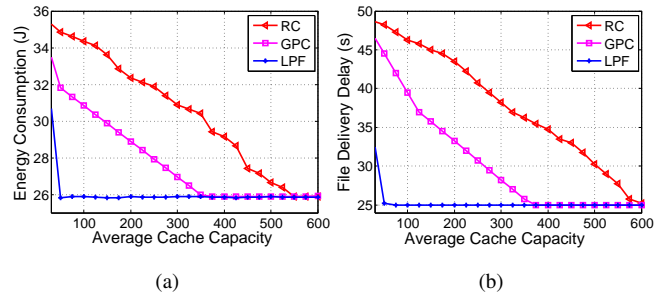


Fig. 5: (a) energy consumption and (b) end-to-end file delivery delay comparison of caching strategies under different average cache capacities

We compare the proposed local popular file placement policy (LPF) with the following caching policies:

- *Global Popularity Caching (GPC)*: It is assumed that the file popularity in DSCNs follows a global popularity distribution. That's to say, all SBSs will cache the global popular files and content in their cache is the same without consideration of cache capacity.
- *Random Caching (RC)*: Each SBS randomly chooses the files to cache regardless of the file popularity distribution.

In Fig. 5, we compare the performance of different caching policies under different average cache capacities at SBSs. The number of user is 150 and α is 0.5. As the average cache capacity increases, LPF achieves the best performance among all three policies. This is due to the fact that the file popularity distribution in different small cells may be different from each other, and the global file popularity distribution does not reflect local file popularity. In detail, for example, in Fig. 5(a) when the average cache capacity measured in the number of files is beyond 50, the energy consumption value obtained by LPF will not decrease. The reason is that each SBS has enough storage to cache all files requested by its local users. But for GPC, each SBS needs much more storage to cache all global popular files (about 350) to satisfy all requests from the local users.

E. Performance Comparison

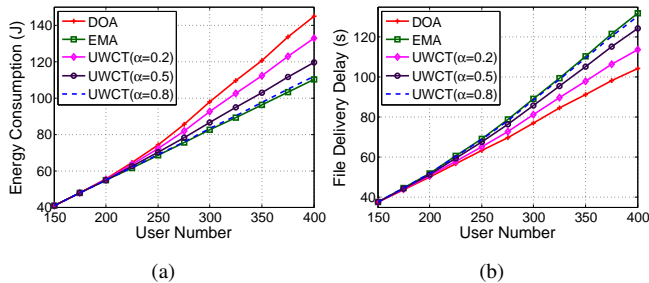


Fig. 6: (a) energy consumption and (b) end-to-end file delivery delay comparison under different numbers of user

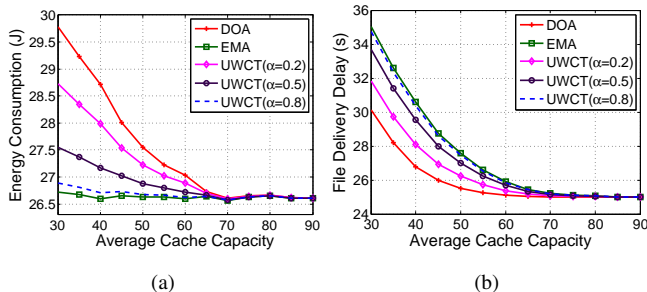


Fig. 7: (a) energy consumption and (b) end-to-end file delivery delay comparison under different cache capacities

To demonstrate the advantages of the proposed energy-delay tradeoff strategy in cache-enabled DSCNs, we refer to the delay-optimal and energy-minimum algorithm under different numbers of users and cache capacities.

- *Delay-Optimal Algorithm (DOA)*: In order to minimize end-to-end file delivery delay, a user will only associate with the SBS caching the requested file from its SBS neighbourhood [2]. This procedure will repeat until no more delay increases.

- *Energy-Minimum Algorithm (EMA)*: In the system model, each user is associated with the closest SBS, and the SBS chooses the most local popular contents in its cache [8].

In Fig. 6, we compare the three algorithms in terms of energy consumption and end-to-end file delivery delay by varying the number of users. The average capacity is 15. In Fig. 6(a), as expected, EMA consumes least energy. The proposed UCWT algorithm consumes more energy than EMA, but always less than DOA. In Fig. 6(b), as expected, DOA achieve minimum end-to-end file delivery delay. UCWT results in higher end-to-end file delivery delay than DOA, but always lower than EMA. This is due to the fact that EMA focuses on energy consumption minimization, which sacrifices end-to-end file delivery delay. It is opposite for DOA that focuses on optimizing delay. We can also see that UCWT can obtain a balance between energy consumption and end-to-end file delivery delay by adjusting tradeoff parameter α . For example, when α is smaller, lower end-to-end file delivery delay is achieved while more energy is consumed.

In Fig. 7, we compare the three algorithms in terms of energy consumption and end-to-end file delivery delay by changing the average cache capacity. The number of user is 150. In Fig. 7(a), the energy consumption value obtained by EMA is almost constant over different average cache capacities. The reason is that users only associate with nearest SBSs without consideration of cached files at SBSs. In Fig. 7(b), compared with EMA and UCWT, DOA achieves minimum end-to-end file delivery delay. From Fig. 7(a) and Fig. 7(b), when the average cache capacity is large enough, both minimum end-to-end file delivery delay and energy consumption are achieved by the three algorithms. This is due to the fact that all users can get required files from their local nearest SBSs.

VI. CONCLUSION

In this paper, we study energy consumption and end-to-end file delivery delay tradeoff problem in cache-enabled DSCNs, where file caching, user association and power control are jointly considered. To solve the problem, firstly, a local popular file placement policy is proposed to maximize the caching hit probability at SBSs. With the proposed file placement policy, the tradeoff problem is further decomposed with Benders' decomposition method. Extension simulations show the proposed algorithms can obtain the desired energy-delay tradeoff under various scenarios.

In the future, we will extend our work to the mobility environments. Furthermore, machine learning based mechanisms will be considered to estimate the file popularity distribution at SBSs.

APPENDIX A
PROOF OF THE PROPOSITION 4

Based on the definition in (24), objective (19) can be equivalently transformed to

$$\begin{aligned} \min_{\eta, \mathbf{X}} \quad & \alpha\eta + (1 - \alpha) \sum_{i=1}^U \sum_{j=1}^B \sum_{k=1}^F \theta_{ik} d_{ij}^k x_{ij}, \\ \text{s.t.} \quad & x_{ij} \in [0, 1], \forall i \in U, \forall j \in B, \\ & \sum_{i=1}^U \sum_{j=1}^B x_{ij} - x_{ij}^2 \leq 0, \end{aligned} \quad (26)$$

remaining constraints is the same as in (19).

The Lagrangian function of (26) with only one Lagrangian multiplier $\lambda \geq 0$ (which leads to (25)) is

$$\begin{aligned} \mathcal{L}(\eta, \mathbf{X}, \lambda) := & \alpha\eta + (1 - \alpha) \sum_{i=1}^U \sum_{j=1}^B \sum_{k=1}^F \theta_{ik} d_{ij}^k x_{ij} \\ & + \lambda \sum_{i=1}^U \sum_{j=1}^B (x_{ij} - x_{ij}^2) \end{aligned} \quad (27)$$

The optimization problem (19) can be expressed by $\min_{(\eta, \mathbf{X})} \max_{\lambda \geq 0} \mathcal{L}(\eta, \mathbf{X}, \lambda)$ (29). According to the duality theory in [26]. So

$$\sup_{\lambda} \phi(\lambda) = \sup_{\lambda} \min_{(\eta, \mathbf{X})} \mathcal{L}(\eta, \mathbf{X}, \lambda), \quad (28)$$

$$\begin{aligned} & \leq \min_{\eta, \mathbf{X}} \max_{\lambda} \mathcal{L}(\eta, \mathbf{X}, \lambda), \quad (29) \\ & = \min(19), \end{aligned}$$

where $\phi(\lambda) = \min_{(\eta, \mathbf{X})} \mathcal{L}(\eta, \mathbf{X}, \lambda)$ and $\phi(\lambda)$ is function over λ . When $\sum_{i=1}^U \sum_{j=1}^B x_{ij} - \sum_{i=1}^U \sum_{j=1}^B x_{ij}^2 \geq 0$ for $x_{ij} \in [0, 1], \forall i, j$, $\mathcal{L}(\eta, \mathbf{x}, \lambda)$ is monotonically increasing over λ for $\forall \mathbf{X} \in \mathbf{A}, \forall \eta$, then $\phi(\lambda)$ is increasing in λ and bounded by the optimal value of (19). Let the optimal solution for (28) is denoted by λ^*, η^* and \mathbf{X}^* , where $\lambda^* \in (0, +\infty)$. Then, the following two cases should be analyzed for the optimal solution of (28).

- The first case is when $\sum_{i=1}^U \sum_{j=1}^B x_{ij}^{(*)} - \sum_{i=1}^U \sum_{j=1}^B (x_{ij}^{(*)})^2 = 0$. At this time, η^* and \mathbf{X}^* are still feasible to (19). Then, when $\eta = \eta^*$ and $\mathbf{X} = \mathbf{X}^*$, we have

$$\begin{aligned} \phi(\lambda^*) &= \mathcal{L}(\eta^*, \mathbf{X}^*, \lambda^*) \\ &= \alpha\eta^* + (1 - \alpha) \sum_{i=1}^U \sum_{j=1}^B \sum_{k=1}^F \theta_{ik} d_{ij}^k x_{ij}^* \quad (30) \\ &\geq \min(19), \end{aligned}$$

Look back at (28) and (30), such following equation holds:

$$\sup_{\lambda} \min_{(\eta, \mathbf{X})} \mathcal{L}(\eta, \mathbf{X}, \lambda) = \min_{\eta, \mathbf{X}} \max_{\lambda} \mathcal{L}(\eta, \mathbf{X}, \lambda),$$

when $\sum_{i=1}^U \sum_{j=1}^B x_{ij} - \sum_{i=1}^U \sum_{j=1}^B (x_{ij})^2 = 0$.

As $\phi(\lambda)$ is monotonically increasing function over λ . Then

$$\phi(\lambda) = \min(19), \forall \lambda \geq \lambda^* \quad (31)$$

Namely, (25) and (19) share the same optimal solutions and value, where $\sum_{i=1}^U \sum_{j=1}^B x_{ij} - \sum_{i=1}^U \sum_{j=1}^B (x_{ij})^2 = 0$. Thus, proposition (4) holds for $\sum_{i=1}^U \sum_{j=1}^B x_{ij} - \sum_{i=1}^U \sum_{j=1}^B (x_{ij})^2 = 0$.

- The second case is that we assume $\sum_{i=1}^U \sum_{j=1}^B x_{ij} - \sum_{i=1}^U \sum_{j=1}^B (x_{ij})^2 > 0$, $\lambda > 0$ for optimizing (28). Due the monotonicity of function $\phi(\lambda)$ over λ , $\max_{\lambda \geq 0} \phi(\lambda)$ tends to $+\infty$ with $\lambda \rightarrow +\infty$. Such result contradicts the conclusion that (28) is less than the optimal value of (19) in expression (29). Thus, there exists \hat{x}_{ij} satisfying $\sum_{i=1}^U \sum_{j=1}^B \hat{x}_{ij} - \sum_{i=1}^U \sum_{j=1}^B (\hat{x}_{ij})^2 = 0$ with $\lambda \rightarrow +\infty$.

Based on the above analysis, we can conclude that when an appropriate value is chosen for λ , the problem (19) is equivalent to the problem (25) in the sense that they share the same optimal value as well as optimal solution.

REFERENCES

- [1] P. Blasco, D. Gndz, "Learning-based optimization of cache content in a small cell base station," in *Proc. IEEE ICC*, Sydney, NSW, 2014, pp. 1897-1903.
- [2] H. Zhang, Y. Chen, Z. Yang and X. Zhang, "Flexible Coverage for Backhaul-Limited Ultra-Dense Heterogeneous Networks: Throughput Analysis and η -Optimal Biasing," *IEEE Trans. Veh. Technol.*, vol. PP, no. 99, pp. 1-1, 2018.
- [3] D. Liu, B. Chen, C. Yang and A. F. Molisch, "Caching at the wireless edge: Design aspects, challenges, and future directions," *IEEE Commun. Mag.*, vol. 54, no. 9, pp. 22-28, 2016.
- [4] B. N. Bharath, K. G. Nagananda and H. V. Poor, "A Learning-Based Approach to Caching in Heterogenous Small Cell Networks," *IEEE Trans. Commun.*, vol. 64, no. 4, pp. 1674-1686, April 2016.
- [5] D. Liu, C. Yang, "Energy efficiency of downlink networks with caching at base stations," *IEEE J. Sel. Areas Commun.*, vol. 34, no. 4, pp. 907-922, 2016.
- [6] M. Dehghan, A. Seetharam ,B. Jiang, "On the complexity of optimal routing and content caching in heterogeneous networks," in *Proc. IEEE INFOCOM*, Kowloon, 2015, pp. 936-944.
- [7] K. Poularakis, G. Iosifidis, A. Argyriou and L. Tassiulas, "Video delivery over heterogeneous cellular networks: Optimizing cost and performance," in *Proc. IEEE INFOCOM*, Toronto, ON, 2014, pp. 1078-1086.
- [8] K. Guo, C. Yang and T. Liu, "Caching in Base Station with Recommendation via Q-Learning," in *Proc. IEEE WCNC*, San Francisco, CA, 2017, pp. 1-6.
- [9] X. Ge, J. Yang, H. Gharavi and Y. Sun, "Energy Efficiency Challenges of 5G Small Cell Networks," *IEEE Commun. Mag.*, vol. 55, no. 5, pp. 184-191, May 2017.
- [10] A. Mesodiakaki, F. Adelantado, L. Alonso and C. Verikoukis, "Energy-efficient user association in cognitive heterogeneous networks," *IEEE Commun. Mag.*, vol. 52, no. 7, pp. 22-29, July 2014.
- [11] H. Zhang, S. Huang, C. Jiang, K. Long, V. C. M. Leung, H. V. Poor, "Energy efficient user association and power allocation in millimeter wave based ultra dense networks with energy harvesting base stations", *IEEE J. Sel. Areas Commun.*, vol. PP, no. 99, pp. 1-1, 2017.
- [12] Cisco, Visual Networking Index, "Forecast and Methodology, 2015-2020," Jun. 2016.
- [13] W. Zhang, Y. Wen, Z. Chen, A. Khisti, "QoE-Driven Cache Management for HTTP Adaptive Bit Rate Streaming Over Wireless Networks," *IEEE Trans. Multimedia*, vol. 15, no. 6, pp. 1431-1445, Oct. 2013.
- [14] J. G. Andrews, S. Buzzi, W. Choi et al., "What Will 5G Be?," *IEEE J. Sel. Areas Commun.*, vol. 32, no. 6, pp. 1065-1082, June 2014.

- [15] M. Zink, K. Suh, Y. Gu, and J. Kurose, "Watch global cache local: YouTube network traces at a campus network-Measurements and implications," in *Proc.ACM Multimedia Comput. Netw.*, SantaClara, CA, USA, 2008.
- [16] B. Chen and C. Yang, "Caching Policy Optimization for D2D Communications by Learning User Preference," in *Proc. IEEE VTC Spring*, Sydney, NSW, 2017, pp. 1-6.
- [17] D. C. Chen, T. Q. S. Quek and M. Kountouris, "Backhauling in Heterogeneous Cellular Networks: Modeling and Tradeoffs," *IEEE Trans. Wireless Commun.*, vol. 14, no. 6, pp. 3194-3206, June 2015.
- [18] R. T. Marler and J. S. Arora, "Survey of multi-objective optimization methods for engineering," *Struct. Multidisc. Optim.*, vol. 26, pp. 369C395, 2004.
- [19] K. Kato and M. Sakawa, "Genetic algorithms with decomposition procedures for multidimensional 0-1 knapsack problems with block angular structures," *IEEE Trans. Syst. Sci. Cybern.*, vol. 33, no. 3, pp. 410-419, June 2003.
- [20] A. Fréville, "The multidimensional 0-1 knapsack problem: An overview," *Eur. J. Oper. Res.*, vol. 155, no. 1, pp. 1-21, 2004.
- [21] E. Bastug, M. Bennis and M. Debbah, "Living on the edge: The role of proactive caching in 5G wireless networks," *IEEE Commun. Mag.*, vol. 52, no. 8, pp. 82-89, Aug. 2014.
- [22] A. Liu and V. K. N. Lau, "Mixed-Timescale Precoding and Cache Control in Cached MIMO Interference Network," *IEEE Trans. Signal Process.*, vol. 61, no. 24, pp. 6320-6332, Dec.15, 2013.
- [23] M. Tao, E. Chen, H. Zhou and W. Yu, "Content-Centric Sparse Multicast Beamforming for Cache-Enabled Cloud RAN," *IEEE Trans. Wireless Commun.*, vol. 15, no. 9, pp. 6118-6131, Sept. 2016.
- [24] J. F. Benders, "Partitioning procedures for solving mixed-variables programming problems," *Numerische mathematik*, vol. 4, no. 1, pp. 238-252, 1962.
- [25] M. Dale, M. Devine, "A modified Benders' partitioning algorithm for mixed integer programming," *Management Science*, vol. 24, no. 3, pp. 312-319, 1977.
- [26] D. Bertsimas, J. N. Tsitsiklis. "Introduction to linear optimization". Belmont, MA: Athena Scientific, 1997.
- [27] D. H. Dirk, "Interior point approach to linear, quadratic and convex programming: algorithms and complexity," *Springer Science & Business Media*, 2012.
- [28] B. J. Rosen, M. P. Pardalos, "Global minimization of large-scale constrained concave quadratic problems by separable programming," *Numerische mathematik*, vol. 34, no. 2, pp. 163-174, 1986.
- [29] Y. Yu, E. Dutkiewicz, X. Huang and M. Mueck, "Downlink Resource Allocation for Next Generation Wireless Networks with Inter-Cell Interference," *IEEE Trans. Wireless Commun.*, vol. 12, no. 4, pp. 1783-1793, April 2013.
- [30] 3GPP TR 36.819 v11.0.0, "Coordinated Multi-Point Operation for LTE," 3GPP TSG RAN WG1, Sept. 2011.
- [31] D. W. K. Ng, Y. Wu and R. Schober, "Power Efficient Resource Allocation for Full-Duplex Radio Distributed Antenna Networks," *IEEE Trans. Wireless Commun.*, vol. 15, no. 4, pp. 2896-2911, April 2016.